Interaction of Hg overlayers with an Ag(100) surface

P. A. Dowben, Y. J. Kime, and Shikha Varma
Department of Physics, Syracuse University, Syracuse, New York 13244

M. Onellion* and J. L. Erskine
Department of Physics, University of Texas, Austin, Texas 78712
(Received 13 November 1986)

The electronic band structure of one, two, and five monolayers of Hg on Ag(100) has been investigated by angle-resolved photoemission. Hg overlayers on Ag(100) form metastable structures that develop via Frank–van der Merwe growth modes. Hg-Hg hybridization results in the formation of a two-dimensional band structure while hybridization of Hg with the underlying Ag(100) substrate results in the adoption of bulklike characteristics for some Hg-induced bands. The Hg-Hg as well as Hg-Ag interactions are discussed.

I. INTRODUCTION

Within the last several years, researchers have begun investigating metal overlayers of a few monolayers thickness.[1–3] The motivations have included experimental tests of two-dimensional system properties,[3–5] epitaxial-growth mechanisms,[6] and interfacial states between the substrate and overlayer.[7,8] Previous investigations have included noble-[9] and transition-metal[10] overlayers.

A special class of metal overlayer systems involves the closed-shell metals, i.e., those metals in the II*A* and II*B* columns of the Periodic Table. Such systems are expected to possess several interesting features as a result of the electronic configuration of the II*A* and II*B* metals. Hybridization and many-electron effects are more readily identified for these metals, by virtue of their closed atomic orbitals. Several such elements possess, in their photoemission spectra, energy levels commonly regarded as shallow core levels. Shallow core levels have been generally regarded as virtually atomic and, hence, not thoroughly investigated.[11,12] However, if the shallow core levels are sufficiently close in binding energy to the valence-band states of the substrate, then interfacial states that include the shallow core levels are possible. Finally, the II*A* and II*B* elements in many cases possess lattice constants close to those of noble- or transition-metal substrates, so that epitaxial overlayers can be grown.

In this work we selected the metal-on-metal adsorption system of Hg on Ag(100). This choice of adsorbate and substrate offers a number of advantages. The Hg lattice constant is only slightly larger ($\sim 3.8\%$) than that of Ag(100). Hg exhibits a spin-orbit doublet that, at binding energies of ~ 8 and ~ 10 eV is reasonably close to the Ag *d* bands. Ag is a chemically inert metal, and it is reasonable to expect that Ag(100) would provide a structural template for Hg, without a significant hybridization of electronic states, though some influence of the Ag *d* band should be observed in the Hg overlayer. We examined thin Hg films of varying thickness adsorbed on Ag(100) with low-energy electron diffraction (LEED), Auger electron spectroscopy, and angle-resolved photoemission spectroscopy (ARPES). In the work reported herein, we have characterized some unusual properties of the interfacial states that arise as a result of mixing Hg and Ag electronic states. Thin-film metal overlayers do not simply contribute new two-dimensional electronic states, and alter surface states of the substrate.

II. EXPERIMENTAL

The angle-resolved photoemission spectra were obtained in an ultrahigh-vacuum (UHV) system equipped with a retarding analyzer for LEED and Auger electron spectroscopy as well as a hemispherical analyzer for ARPES described elsewhere.[11] The light source for photoemission was the Tantalus I synchrotron dispersed by a 3-m toroidal-grating monochrometer. The energy resolution of the photoemission spectra collected by the hemispherical analyzer varied from 0.15 to 0.4 eV full width at half maximum (FWHM), including the resolution of the photon source. Relative photoemission intensities were estimated from the integral counts for a photoemission feature and normalized by the electron beam current in the synchrotron and the transmission of the monochromator, as described elsewhere,[12] unless stated otherwise. The operating mode of the hemispherical analyzer used for photoemission yielded a constant transmission, as shown by ray tracing and transmission measurements.[13] The electric vector potential **A** of the incident light was parallel to the surface and the Ag $\langle 1\bar{1}0 \rangle$ direction throughout this work (the $\bar{\Gamma}$-to-$\bar{X}$ direction of the surface Brillouin zone).

Throughout this work, odd (even) geometry refers to placing the electron energy analyzer so as to collect electrons in the plane perpendicular to (parallel to) the plane defined by the surface normal and the vector potential **A**. This is defined in this manner because the electron initial-state wave function has odd (even) reflection symmetry with respect to this plane.

The surface contamination following cleaning and annealing of the Ag(100) surface was characterized by LEED and Auger electron spectroscopy and was less than

1% of a monolayer. The Ag(100) surface was cleaned by 500-eV Ar^+-ion bombardment and carefully annealed so that a sharp 1×1 LEED pattern was observed. The Ag(100) crystal was cooled to 89 K (as determined using a Chromel-Alumel thermocouple), following cleaning and annealing, using a liquid-nitrogen cold stage. Triply distilled Hg was admitted to the chamber via a standard variable-leak valve. Contamination (apart from Hg) following adsorption of Hg on the surface at 89 K was less than the detection limit (1 at.%) of our Auger electron spectrometer.

The photoemission spectra shown in this manuscript are the raw spectra uncorrected for background and noise. No smoothing functions or deconvolution procedures have been applied in the analysis of this data. Unless otherwise stated, all the Hg films were formed with the Ag(100) substrate at 89 K and an ambient Hg pressure of 10^{-8} Torr or less. We selected such a low ambient Hg pressure for deposition to reduce the possibility of Hg-Ag amalgamation.

III. RESULTS AND DISCUSSION

There are several questions to answer in any investigation of metal-on-metal overlayer deposition. The major questions concern the dominant growth mode, the extent and existence of long-range order, and the electronic band structure. In addition to investigating these questions, we have also made measurements to determine the extent of alloying between the Hg and the Ag(100) surface. In separate sections, we address the issues of the Hg overlayer growth kinetics on Ag(100), the long-range order as a function of film thickness, and the electronic band structure.

A. Adsorption and growth of Hg-overlayer thin films on Ag(100) at 89 K

We have observed that Hg adsorbs readily on Ag(100) at 89 K. By contrast, the same exposure of Hg to Ag(100) at 300 K results in less Hg adsorption by some 200 times than at 89 K. Furthermore, Hg adsorbed on Ag(100) at 89 K desorbs upon raising the temperature to 300 K. We have investigated desorption of Hg following Hg adsorption at 89 K, as detailed elsewhere,[14] and found that Hg desorbs resulting in a monotonically decreasing coverage with increasing temperature. This strongly suggests that Hg overlayers on Ag(100) are weakly bound. Hg overlayers on W(100) (Refs. 15 and 16) and Fe(100) (Ref. 17) have also been characterized as weakly bound, with heats of adsorption of 208 ± 12 kJ/mol and 109 ± 12 kJ/mol, respectively, and with desorption temperatures well above that for Hg on Ag(100). Indeed, Hg does not readily adsorb on either Ag(100) or Au. Some 1.8×10^6 L Hg exposure (one langmuir$=1$ L$=10^{-6}$ Torr s) to an Au film at room temperature resulted in only modest Hg adsorption, observed via small Hg photoemission intensities detected following exposure.[18]

The apparent low energy of desorption for Hg from Ag(100) indicates that amalgamation does not occur with Hg adsorption on Ag(100) at 89 K and Hg vapor pressure less that 10^{-8} Torr. The absence of alloying under these conditions is also supported by evidence provided by the relative Hg and Ag photoemission feature intensities discussed below. The absence of Hg amalgamation with Ag(100) at 89 K indicates that the activation barrier for Hg diffusion into the Ag crystal cannot be overcome at this low temperature and ambient pressures less than 10^{-8} Torr.

We investigated the growth mode of Hg overlayers on Ag(100) using Auger electron spectroscopy (AES) and photoemission. The ratio of the Hg 242-eV AES feature to the Ag 264-eV AES feature as a function of exposure was found to increase linearly up to 3 L exposure. These results indicated that the Hg adsorbs on Ag(100) at 89 K with a constant sticking coefficient for the first layer. The ratio of the Hg and Ag photoemission feature intensities as a function of Hg exposure has also been measured for photon energies of 25, 30, 40, and 50 eV. The development of the Hg-induced photoemission features and the attenuation of the Ag photoemission features are shown in Figs. 1 and 2. Leaving the discussion of the electronic structure for a subsequent section (*vide infra*), consider the Hg feature labeled *A* and *B* and the Ag photoemission feature labeled *C*. As illustrated in Fig. 3(a), the ratios of the integral intensities of the photoemission features *A* to *C* and *B* to *C* increase linearly with initial exposure, as expected if the initial adsorption results in a complete monolayer of Hg.

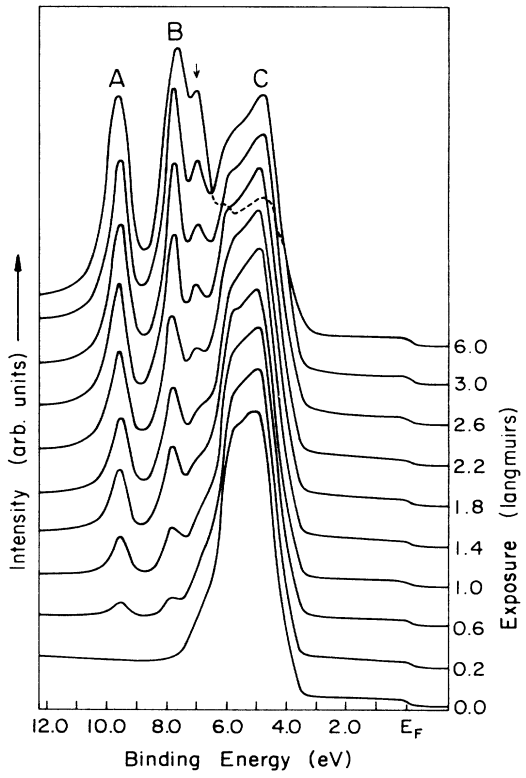

FIG. 1. Normal-emission photoelectron energy distribution curves ($h\nu=50$ eV) for various exposures of Hg (in langmuirs) on Ag(100) at 89 K. The vector potential of the incident light is parallel to the $\langle 1\bar{1}0\rangle$ direction of the Ag(100) surface. Arrow denotes new feature.

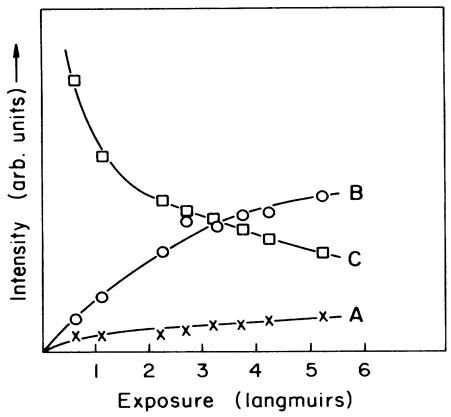

FIG. 2. The intensity of photoemission features (indicated in Fig. 1) A (x), B (○), and C (□), as a function of Hg exposure to Ag(100) at 89 K.

The adsorption data is consistent with layer-by-layer growth of the Hg overlayer. The increasing slope in the ratio of Hg photoemission signal to the Ag photoemission signal, as shown in Fig. 3(b), suggests that the Hg adsorbs evenly over the surface. An Hg overlayer adsorption process that leads to a "hill and valley" structure of the overlayer [thick and thin islands of Hg on Ag(100)] would result in a Hg-to-Ag signal ratio that tends toward a constant value with increasing Hg exposure. This is neither observed in photoemission at photon energies of 25, 30, 40, and 50 eV, nor observed using Auger electron spectroscopy. Hg amalgamation with a Ag(100) surface would also lead to an Hg-to-Ag electron spectroscopy signal ratio that approaches a constant value with continued Hg exposure; thus, these results also argue against alloying of Hg with the Ag(100) substrate.

The attenuation of the Ag d-band photoemission features with Hg exposure, at photon energies of 25, 30, 40, and 50 eV (corrected for the synchrotron beam current) and using constant-analyzer-transmission conditions, is exponential. This signal attenuation, together with the electron mean-free paths of Seah and Dench,[19] Penn,[20] and Powell[21] indicates that an Hg monolayer is adsorbed on Ag(100) at 89 K following 2.6 to 3.0 L Hg exposure. Two monolayers of Hg are adsorbed on Ag(100) following approximately 6 L Hg exposure while six to seven monolayers of Hg are adsorbed following 20 L Hg exposure. Thus, we conclude from the above results that layer-by-layer growth is dominant in the coverage range up to seven monolayers.

While the growth of the Hg film on Ag(100) appears to follow a Frank–van der Merwe growth mode (layer by layer),[22,23] some Stranski-Krastanov growth cannot be completely excluded (growth of three-dimensional crystals on a six- to seven-monolayer film of Hg). This implies that

$$\Delta\varepsilon=\sigma_f+\sigma_i-\sigma_s\leq 0,\quad \sigma_s\geq\sigma_f+\sigma_i\ , \tag{1}$$

where σ_f and σ_s are the specific free energies of the film and substrate respectively, and σ_i is the specific free interfacial energy.

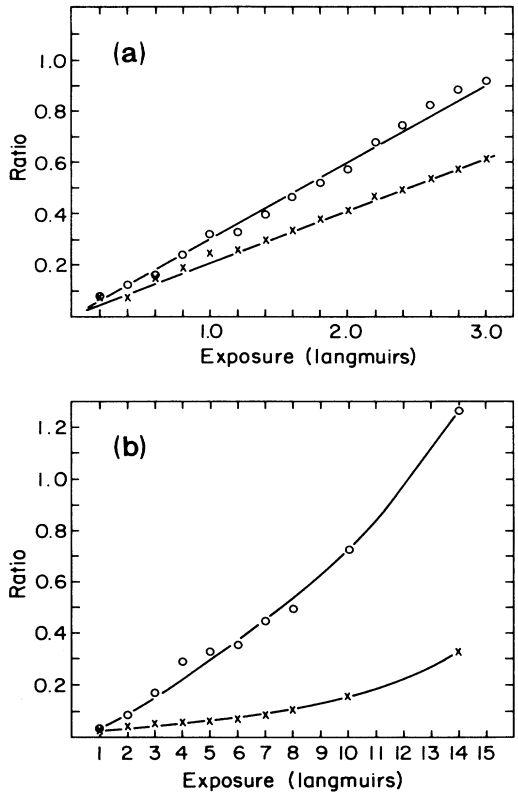

FIG. 3. The ratio of the Hg $5d_{5/2}$ photoemission intensity relative to the intensity of the Ag $4d$ bands is a function of exposure to Hg vapor. The Ag(100) substrate is at 89 K. The photon energy in Fig. 3(a) is 50 eV, while the photon energy for the ratio of intensities in Fig. 3(b) is 25 eV. Data was taken from photoemission spectra similar to those plotted in Fig. 1. ○ indicates the ratio of photoemission features A:C, while x indicates the ratio of photoemission features B:C.

Only two distinct low-energy electron diffraction patterns have been observed for Hg adsorption on Ag(100) at 89 K for exposures of less than 40 L Hg. Up to 7 L Hg exposure, the 1×1 LEED pattern is observed as shown schematically in Fig. 4. With exposure beyond 7 L the LEED pattern reflections become increasingly diffuse and the diffraction pattern (if any) is increasingly difficult to determine. At about 14 L Hg exposure, a second LEED pattern is observed as shown in Fig. 4. For 40 L or more Hg exposure, a third LEED pattern is occasionally observed. This third LEED pattern is attributed to the development of the bulk Hg crystal structure.

For one and two monolayers of Hg on Ag(100) at 89 K (3 and 6 L Hg exposure, respectively), the LEED results indicated that the Hg monolayer adopts the fcc 1×1 lattice of the Ag(100) substrate. This epitaxial growth of one and two monolayers of Hg on Ag(100) is not surprising. Mercury adlayers adopt the 1×1 crystal lattice of the substrate for both W(100) (Refs. 15 and 16) and Fe(100) (Ref. 17). The bcc lattice constant for Fe(100) at 2.87 Å is nearly identical to the fcc lattice constant for Ag(100) at 2.889 Å. Thus a similarity of the epitaxial growth behav-

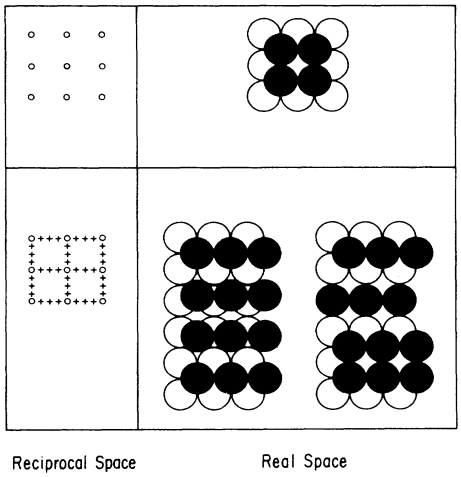

FIG. 4. The schematic reciprocal space nets for one and two monolayers of Hg on Ag(100) are shown (top) as well as the reciprocal space nets for five to seven monolayers of Hg on Ag(100) (bottom). The 1×1 overlayer (top) for Hg has been drawn with the Hg atoms (black) of the outermost layer resting in the fourfold hollow of the layer below—though no evidence as to site yet exists. Two possible solutions for the structure for five to seven monolayers of Hg are shown (black) with the 1×1 lattice indicated in white.

ior on Ag(100) and Fe(100) is not surprising.

As Hg coverage increased beyond two monolayers, the LEED pattern deteriorated monotonically until by ~4 monolayers there was no LEED pattern. The 1×1 Hg lattice for one and two monolayers of Hg on Ag(100) is an artificial and metastable structure. The fcc lattice is not the natural rhombohedral (α-phase) crystal structure of bulk mercury for which the nearest-neighbor lattice constant is 3.004 Å (Refs. 24–28) (or 2.993 Å in the face-centered rhombohedral lattice at 77 K).[24]

Weaire[25,27] and Heine and Weaire[26] point out that the Hg crystal structures exhibit an instability of the fcc structure with respect to rhombohedral distortion, and metastability with respect to tetragonal distortion. The energy of the fcc Hg lattice is close to the energy of the rhombohedral lattice as shown by Worster and March, who calculated only a 0.01 eV per atom difference.[29] Thus, for one and two monolayers of Hg on Ag(100), the Hg overlayer lattice constant is a compression of 3.5–3.8 % from the Hg lattice constant for bulk Hg. This means that the Hg overlayer lattice is a strained lattice. With increasing overlayer thickness, defects will occur in the epitaxial Hg overlayer as a result of this strain. For the third and fourth monolayers of Hg adsorbed on Ag(100) at 89 K, the LEED patterns are indicative of substantial disorder. This disorder is most likely a result of a high concentration of strain-relief-related defects.

With continuing exposure and adsorption beyond four monolayers, we observed the gradual establishment of a new LEED pattern, as shown schematically in Fig. 4. The LEED results are insufficient to permit a unique assignment of the diffraction pattern to a solution for the overlayer lattice. The overlayer lattices shown in Fig. 5 provide two possible solutions to the observed diffraction pattern. Domains of $p(1\times4)$ overlayer (shown in Fig. 4) could create the observed diffraction pattern, which is interpreted as a superposition of $p(1\times4)$ and $p(4\times1)$ LEED patterns. One of these postulated overlayers has Hg lattice constants of 4.568 Å and 2.889 Å. The other $p(1\times4)$ real-space overlayer net has a rectangular lattice of spacings of 3.852 and 2.889 Å. This observed structure for Hg adsorbed on Ag(100) is similar to the body-centered tetragonal (β-phase) lattice of bulk mercury with rectangular lattice parameters of 2.825 and 3.995 Å (Ref. 24) and suggests that five (or more) monolayers of Hg,

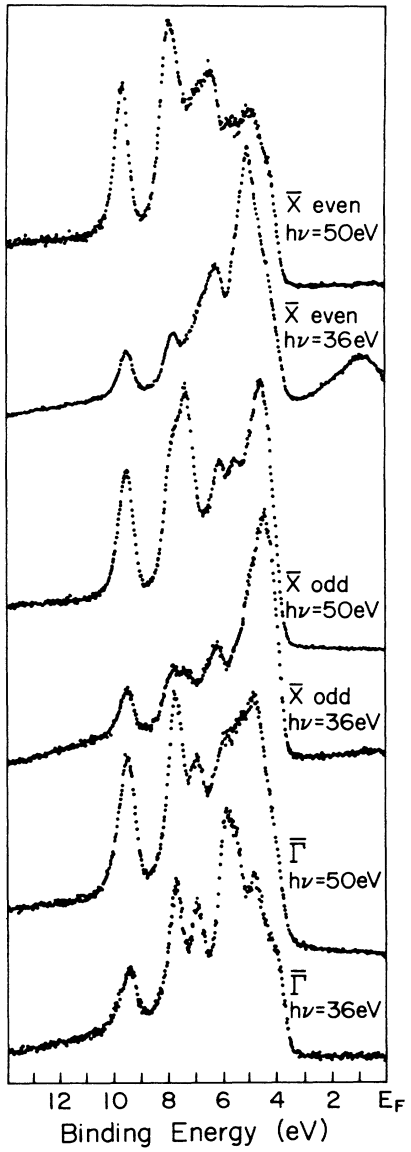

FIG. 5. The emission-angle dependence of the photoemission features for Ag(100) at 89 K following 3 L exposure of Hg vapor. The electric vector potential **A** is in the $\langle 1\bar{1}0\rangle$ direction, corresponding to the $\bar{\Gamma}$-to-$\bar{X}$ direction of the surface Brillouin zone. Both even and odd geometry are shown for emission angles that correspond to the surface Brillouin-zone edge ($\bar{X}$), i.e., 27° off normal for 36 eV incident photon energies and 20° off normal emission for 50 eV incident photon energies.

with the $p(1\times4)$ structure, resemble the high-pressure β phase of bulk mercury. Nonetheless both 3.474- and 3.004-Å lattice spacings occur in the face-centered rhombohedral unit cell of bulk crystalline Hg.[25–27] Indeed, one crystal plane contains these lattice spacings in a rectangular net not unlike one of the proposed real-space solutions to the $p(1\times4)$. A lattice of Hg atoms, however, with a mixture of 3.852-Å (or 4.568-Å) and 2.89-Å lattice constants provides more strain relief than would occur for an overlayer possessing only a 2.889-Å lattice constant. A similar mechanism for strain relief has been proposed for Pb on Cu(100).[6,30] While there are other overlayer structures consistent with the observed diffraction patterns, many of them involve Hg-to-Hg lattice spacings substantially more contracted than the 3.8% contraction the Hg undergoes to produce a 1×1 overlayer at one and two monolayers on Ag(100). Thus, though the LEED patterns permit no conclusive unique assignment, the available evidence suggests that domains of $p(1\times4)$ with lattice spacings of 3.85 and 2.89 Å are the most likely ordered structure for five Hg monolayers. Similar Hg overlayer structures and lattice constants have been observed with Hg adsorption on Ni(100).[31]

There are a number of examples of metal overlayers which grow epitaxially initially, but undergo a structural transformation with increasing thickness of the overlayer.[6] The crystal structure of each succeeding layer will often change as a result of the strain or lattice mismatch of the adsorbate metal with the substrate.

B. The two-dimensional band structure of Hg on Ag(100)

For Hg coverages up to approximately half a monolayer, a doublet feature is evident in the photoemission spectra at $\bar{\Gamma}$ (normal emission) with 8.0±0.2 eV and 9.8±0.1 eV binding energies. This doublet has been attributed to the $5d_{5/2}$ and $5d_{3/2}$ spin-orbit-split states, and has been observed via photoemission for solid Hg,[32,33] Hg adsorbed on Ni(100),[34] W(100),[35] and Au,[18] as well as the gas-phase Hg.[32,36] This assignment is the most likely, although for an atom as heavy as Hg (atomic number of 80), the possibility of a breakdown of the Russell-Saunders angular momentum scheme should be kept in mind.

Following approximately 2 L Hg exposure, a third Hg-induced feature is observed with 7.2±0.1 eV binding energy for normal emission (arrow in Fig. 1). This third Hg-induced feature continues to increase in intensity with increasing Hg adsorption, and is observed with seven-monolayer-thick (20 L) Hg films on Ag(100). This feature has not been observed for bulk solid Hg.[32,33] Similar splittings of the "$5d_{5/2}$-like" have been observed, however, for Hg absorbed on W(100).[35] This further splitting of the $5d_{5/2}$ spin-orbit-split state observed for Hg on W(100) has been attributed[37] to crystal splitting[38] using arguments similar to those proposed by Herbst.[39] For Hg on Ag(100), as will be discussed in detail below, this third feature is not due to crystal-field splitting but rather to the formation of a band structure by the Hg overlayer.[40]

This new feature at 7.2±0.1 eV binding energy only appears with coverages approaching a monolayer. This suggests that this feature is only present when there are adjacent Hg atoms. This is fully consistent with band structure formed from the hybridization of adjacent Hg atom orbitals. As we shall see, this feature can be associated with a two-dimensional band structure. Indeed, we shall demonstrate that this new feature is a result of Hg orbital hybridization forming a distinct Hg band structure.

Using the relationship for the reciprocal momentum vector parallel to the surface, $k_{\parallel}$, for the outgoing photoelectron,

$$k_{\parallel}=0.51(E_{\rm kin})^{1/2}\sin\theta\ , \tag{2}$$

$$E_{\rm kin}=h\nu-E_B-\phi\ , \tag{3}$$

where θ is the emission angle and $E_{\rm kin}$ is the kinetic energy of the electron, i.e., the photon energy minus the binding energy E_B and the work function ϕ. We have mapped out the experimental band structure for one and two

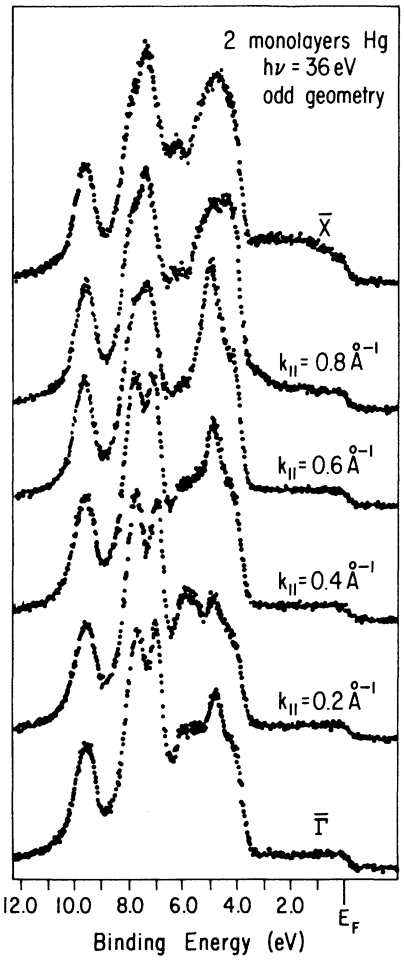

FIG. 6. The emission-angle dependence of the photoemission features for 6 L Hg exposure to Ag(100) at 89 K. The electric vector potential **A** is in the $\langle 1\bar{1}0\rangle$ direction corresponding to the $\bar{\Gamma}$-to-$\bar{X}$ direction of the surface Brillouin zone. The analyzer is collecting the photoelectrons in the plane perpendicular to the vector potential **A** and the surface (odd geometry). The photon energy is 36 eV.

monolayers of Hg on Ag(100) at 89 K from $\bar{\Gamma}$ to $\bar{X}$. The band structure was mapped out from emission-angle-dependent data similar to that shown in Figs. 5–7. There exists emission-angle dependence in the Hg-induced photoemission features following Hg adsorption.

With the electron energy analyzer in odd geometry, the Hg-induced feature with the 7.2±0.1 eV binding energy at normal emission ($\bar{\Gamma}$) disperses to greater binding energies with increasing emission angles for one monolayer of Hg on Ag(100) (3 L), as shown in Fig. 5. The binding energy of this feature increased by 0.36 eV, reaching a maximum of 7.6±0.1 eV at emission angles corresponding to $\bar{X}$ of the square surface Brillouin zone. This feature is not observed away from $\bar{\Gamma}$ in even geometry. The Hg-induced photoemission features, in odd geometry, have binding energies independent of photon energy as well.

The two Hg-induced features at 8.0±0.1 eV and 9.8±0.1 eV binding energies, i.e., the "$5d_{5/2}$- and $5d_{3/2}$-like" spin-orbit-split doublet features, do not disperse substantially with changes in the emission angle for either one monolayer (3 L) or two monolayers (6 L) of Hg on Ag(100) (Figs. 5–7). The ratio of the height of the Hg-induced feature at approximately 7.2 eV binding energy to the $5d_{5/2}$- and $5d_{3/2}$-like bands, however, varies considerably with emission angle in odd geometry for one monolayer of Hg on Ag(100), as shown in Fig. 8. For a photon energy of 50 eV, the (7.2–7.6)-eV photoemission feature increases dramatically (relative to the other Hg-induced photoemission features) with increasing emission angle until about 20° off normal. This corresponds to approximately $\bar{X}$ of the surface Brillouin zone. Emission angles corresponding to values of $k_{\parallel}$ greater than $\bar{X}$ result in a decrease in the relative Hg emission signal for the feature at 7.2–7.6 eV binding energy.

Clearly, one monolayer of Hg adsorbed on Ag(100) not only adopts the 1×1 fcc lattice of the substrate, but yields a two-dimensional band structure consistent with the surface Brillouin zone in odd geometry. This dispersion of the three electronic states attributable to the adsorption of one monolayer of Hg on Ag(100) is indicated in Fig. 9. As stated above, in odd geometry the feature with 7.2 eV binding energy at $\bar{\Gamma}$ disperses to 7.6 eV at $\bar{X}$ and disperses symmetrically about both $\bar{X}$ and $\bar{\Gamma}$. The invariance of the binding energies of the Hg-induced electronic states, in odd geometry, with the changes in photon energy indicate that the electronic states and band structure for one monolayer of Hg on Ag(100) conserve two-dimensionality of state. Conservation of two-dimesionality of state is expected for a band structure formed by a one-atom-thick film.

In addition to the evidence provided by the dispersion of the Hg bands symmetrically about $\bar{\Gamma}$ and $\bar{X}$ in odd geometry, the ratio of the photoemission signal of the 7.2-eV binding-energy feature (at $\bar{\Gamma}$) with respect to the Hg features at 8.0 and 9.8 eV (Fig. 8) also is indicative of band structure. This ratio reaches a maximum at emis-

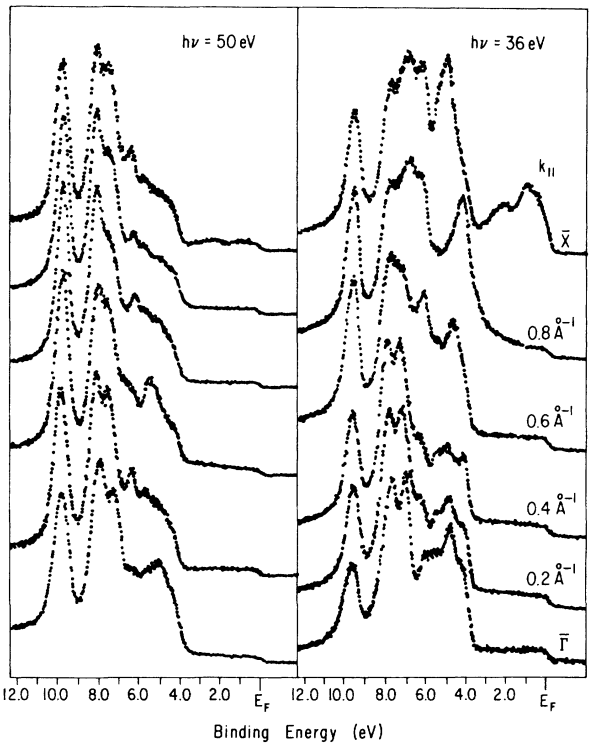

FIG. 7. The emission-angle dependence of the photoemission features of Ag(100) following 6 L Hg exposure (even geometry). The electric vector potential **A** is in the $\langle 1\bar{1}0\rangle$ direction corresponding to the $\bar{\Gamma}$-to-$\bar{X}$ direction of the surface Brillouin zone. The analyzer is collecting the photoelectrons in the plane parallel with the vector potential **A** (even geometry). The right shows emission-angle dependence of the photoemission spectra for 36 eV photon energy and the left shows emission-angle dependence for 50 eV incident photon energy.

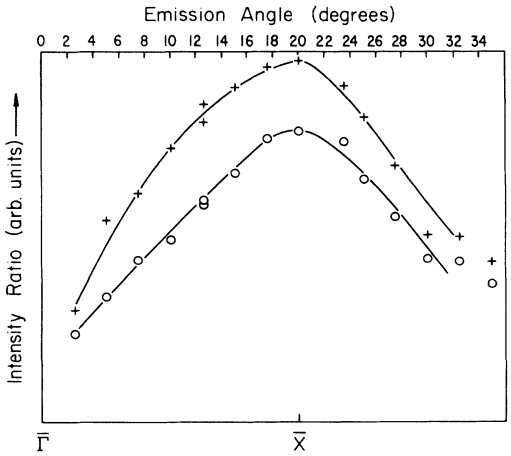

FIG. 8. The relative ratio of the height of the new ~7.2-eV binding energy Hg-induced photoemission feature to the $5d_{5/2}$-orbital Hg photoemission signal with 8.0 eV binding energy (○), and to the $5d_{3/2}$-orbital Hg photoemission signal with ~9.6 eV binding energy (+) as a function of emission angle. The photon energy is 50 eV. The electric vector potential of the incident light is parallel to the surface $\langle 1\bar{1}0\rangle$ direction. The analyzer is collecting the photoelectrons in the plane perpendicular to the surface and electric vector potential **A** (odd geometry). The mercury coverage is approximately one monolayer [3 L Hg on Ag(100) at 89 K].

sion angles corresponding with $\bar{X}$ (Fig. 8). This relative signal intensity indicates that the feature at 7.2 to 7.6 eV binding energy has an intensity that is far greater than the $5d_{5/2}$-like Hg orbitals at $\bar{X}$. Since the (7.2–7.6)-eV band exhibits a band structure that has relatively little dispersion about $\bar{X}$ in the Brillouin zone, one can reasonably expect a greater density of states about $\bar{X}$ and a corresponding increase in photoemission intensity, as is observed. The intensity variation (Fig. 8) is consistent with the two-dimensional crystallography of the surface.

Two monolayers of Hg on Ag(100) also exhibit two-dimensional band structure for odd geometry, and this band structure, moreover, is virtually identical to the band structure observed for one monolayer of Hg on Ag(100) in odd geometry (Fig. 9). Again the band with 7.2 eV binding energy at $\bar{\Gamma}$ disperses to a 7.6 eV binding energy at $\bar{X}$, as shown in Fig. 9 and exhibited by the emission-angle-dependent photoemission spectra (Fig. 6). This band disperses symmetrically about $\bar{X}$ and $\bar{\Gamma}$ and

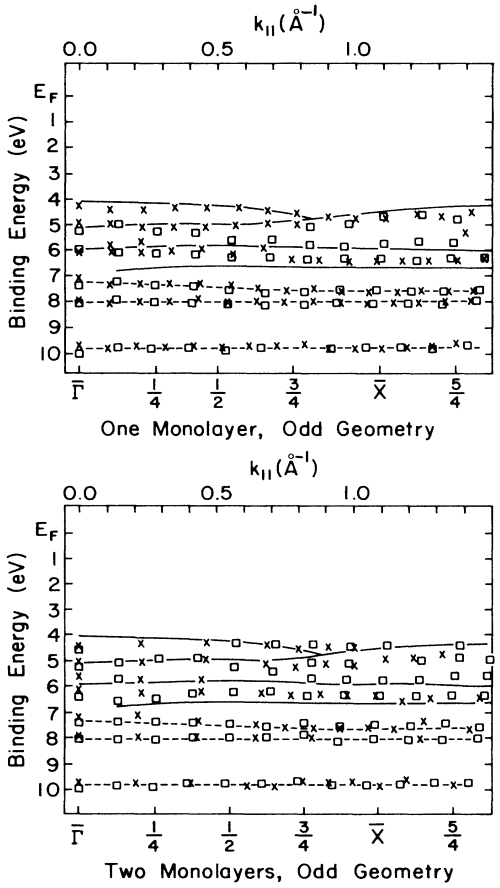

FIG. 9. The experimental band structure of one and two monolayers of Hg on Ag(100), for odd geometry (with respect to the mirror plane). The bands have been mapped out from $\bar{\Gamma}$ to $\bar{X}$ of the surface Brillouin zone (shown in the inset). The experimentally observed bands for clean Ag(100) are indicated by the thin solid lines. Dashed lines indicate the Hg overlayer induced bands, □ indicates data points acquired with a photon energy of 50 eV, while x indicates data points acquired with a photon energy of 36 eV.

conserves two-dimensionality of state (invariance with respect to changes in momentum normal to the surface).

The source of the two-dimensional band structure in odd geometry for one and two monolayers of Hg on Ag(100) must now be addressed. The new Hg feature with 7.2 eV binding energy at $\bar{\Gamma}$ disperses with changes in $k_{\parallel}$ and symmetrically about $\bar{X}$ in odd geometry. Though a similar feature has been observed for Hg absorbed on W(100) (Ref. 35) and attributed to crystal-field splitting[37] using arguments similar to those proposed by Herbst,[39] this explanation is inconsistent with our results for several reasons. This new feature is not observed until an exposure corresponding to more than 0.5 monolayers has been deposited. A crystal-field splitting is unlikely to have this type of coverage dependence. A crystal-field splitting should not vary with a local reduction in the point-group symmetry. In other words, the dispersion of the new 7.2 to 7.6 eV binding-energy feature with $k_{\parallel}$ in odd geometry, symmetrically about $\bar{X}$ and $\bar{\Gamma}$, should not occur with crystal-field splitting. A crystal-field-splitting multiplet of the $5d_{5/2}$ orbital should not exhibit the observed relative intensity dependence of the new feature, with respect to the $5d_{5/2}$ and $5d_{3/2}$ spin-orbit-split doublet, with $k_{\parallel}$ in odd geometry symmetrically about $\bar{X}$ and $\bar{\Gamma}$. Finally, the new feature is observed only in odd geometry away from $\bar{\Gamma}$; it is absent in even geometry for one monolayer of Hg on Ag(100). Such symmetry dependence is difficult to reconcile with crystal-field splitting.

Let us consider the source of this new Hg-induced feature at about 7.2 to 7.6 eV binding energy. The possibility of Hg-Ag alloying was considered in the preceding section but discarded, and cannot be the source of the new feature. An interface state, due to the two materials with different dielectric constants, could form as a result of the establishment of new electronic boundary conditions that produce new electronic states. The possibility that the new feature might be such an interfacial state must also be addressed. We can eliminate this possibility because the new feature becomes more intense with increasing coverage, not less. Following seven monolayers (20 L) Hg adsorption on Ag(100), the new feature at 7.2 eV binding energy was still clearly observable with intensity roughly proportional with the other Hg $5d$ features. The absence of any major Ag electronic state in the photoemission from a seven-monolayer-thick Hg adsorbate argues strongly that this new 7.2-eV binding-energy feature is not a result of Ag contributions.

A clear picture thus emerges in which the Hg-Hg hybridization results in the formation of a third, new $5d$-like Hg photoemission feature with a 7.2 eV binding energy at $\bar{\Gamma}$. This new feature requires sufficient Hg coverage, so hybridization is likely on grounds of geometry, and has virtually identical band structure for one and two monolayers of Hg on Ag(100) for odd symmetry. Since the LEED pattern remains 1×1 for one and two monolayers of Hg, there is a 3.8% reduction in the Hg lattice constant over bulk Hg. Additional Hg-Hg hybridization would accompany such a compression.

The hybridization of adjacent Hg atomic orbitals to form bands is not surprising in view of the close proximity of the Hg atoms in the overlayer lattice. The split-off

Hg $5d$ band is in some respects similar to the third valence d band observed for crystalline Zn.[41] The band structure observed for Hg on Ag(100) is, however, for a metastable structure.

C. The interaction of Hg electronic states with Ag(100)

The emission-angle dependence of the Hg-induced features for one and two monolayers of Hg, in even geometry, is quite different from that observed for odd geometry. We observe that the band structure in even geometry is quite different from the band structure in odd geometry.

In even geometry, the third feature, present at 7.2 ± 0.1 eV binding energy at $\bar{\Gamma}$, is not observed away from $\bar{\Gamma}$ (for emission angles away from the surface normal) for 3 L (one monolayer) Hg on Ag(100) at 89 K (Figs. 5 and 10). For the two monolayers Hg on Ag, the third feature (the (7.2 ± 0.1)-eV binding-energy feature at $\bar{\Gamma}$) is observed. In contrast to odd geometry where the feature disperses symmetrically about $\bar{X}$, the feature in even geometry does disperse, but not symmetrically about $\bar{X}$. Furthermore, in even geometry the binding energy of the feature changes with photon energy (Figs. 7 and 10) in the vicinity of $\bar{X}$.

There are further differences between even and odd geometry for 6 L of Hg on Ag(100) at 89 K. Clean Ag(100) has a Δ_1-symmetry band near $\bar{X}$ that disperses above the Fermi energy along $\bar{\Gamma}$-$\bar{X}$ in even geometry. For two monolayers of Hg, this feature remains; in addition, there is a satellite feature with 1.2 eV greater binding energy which disperses in a similar fashion to the Ag(100) band. As indicated in Fig. 10, the features are unambiguous at 36 eV photon energy. This new band, just as with the Ag(100) Δ_1 band, does *not* disperse symmetrically about $\bar{X}$.

The two monolayers of Hg on Ag(100) show some Hg-induced features in even geometry with band structure that has properties that are quite unusual, and indeed inconsistent with a two-dimensional band structure. First, there exists a dispersion of a band from ~3 eV binding energy at a point $\frac{9}{10}$ of the way from $\bar{\Gamma}$ to $\bar{X}$ to a binding energy close to the Fermi level at a point $\frac{11}{10}$ of the way from $\bar{\Gamma}$ to $\bar{X}$. This dispersion is neither symmetric about $\bar{X}$ nor is it independent of photon energy, as demonstrated in Fig. 10. In addition, the band with 7.2 eV binding energy at $\bar{\Gamma}$ does not disperse symmetrically about $\bar{X}$ either, and again has a dispersion that is influenced by changes in photon energy, as shown in Fig. 10. This clearly indicates that these bands are not conserving the two-dimensionality of states and appear to have the characteristics associated with bulk band structure.

Two monolayers of Hg are of a thickness that is best described as a two-dimensional overlayer. Thus, the bulk-like band-structure characteristics of the two-monolayer Hg film on Ag(100) are suggestive of an admixture of Ag(100) bulk states that exerts a strong influence upon the Hg overlayer band structure. To assess the influence of the Ag(100) band structure upon the Hg overlayer as well as the influence of the overlayer upon the electron structure of the Ag(100) surface, the Ag(100) photoemission features for clean Ag(100), and following one and two monolayers of Hg, have been characterized. The majority of Ag-derived photoemission features disperse in a similar fashion for clean Ag(100) and following adsorption of one (3 L) and two (6 L) monolayers of Hg. Nonetheless, several Ag bands have been shifted in binding energy in comparison to their binding energies for the clean surface, particularly in the vicinity of $\bar{X}$. This pertubation of the Ag(100) bands also suggests some mixing of the Ag and Hg states in the vicinity of $\bar{X}$.

The Ag(100) surface is a C_{4v} surface, both for the clean surface as well as with one and two monolayers of Hg on Ag(100). The surface Brillioun zone retains the symmetry of a C_{4v} surface (fourfold symmetric). This restricts the allowed photoemission states that can be observed at $\bar{\Gamma}$ (normal emission and a C_{4v} symmetry point of the surface Brillioun zone) to Δ_1 or Δ_5 symmetry.[41] The light in-

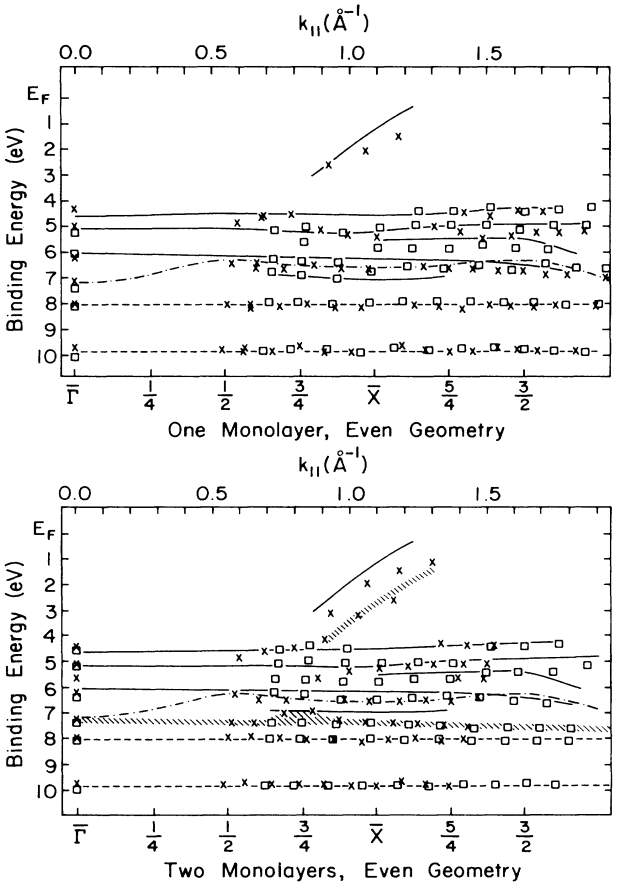

FIG. 10. The experimental band structure for one and two monolayers of Hg on Ag(100), for even geometry. The bands have been mapped out from $\bar{\Gamma}$ to $\bar{X}$ of the surface Brillouin zone. Experimentally observed bands for clean Ag(100) are indicated by the thin solid lines, while the dashed-dotted (— · — · —) lines indicate the Ag(100) calculated band of Δ_1 character (Refs. 43 and 44) and the dashed lines (— — —) indicate the Hg-overlayer-induced bands. Hatched lines \\\\\ indicate Hg bands with substantial hybridization with the underlying Ag(100) substrate (see text). x indicates the data taken with 36 eV photon energy and □ indicates the data acquired with a 50 eV photon energy.

cident on the crystal surface, throughout this work, has the vector potential **A** parallel with the surface. This further restricts the observed photoemission features observed at $\bar{\Gamma}$ to be of Δ_5 symmetry.

The 7.2-, 8.0-, and 9.8-eV binding-energy features of $\bar{\Gamma}$ induced by one and two monolayers of Hg on Ag(100) are observed with binding energies close to those expected for the spin-orbit-split doublet of Hg $5d_{5/2}$ and $5d_{3/2}$. These three photoemission features are therefore expected to be of largely $d_{xz,yz}$ character of $\bar{\Gamma}$. The dispersion of the 7.2-eV binding-energy feature at $\bar{\Gamma}$ to the greater binding energy of 7.6 eV at $\bar{X}$, in odd geometry, is consistent with the expected tight-binding approximation model for dispersion of a Δ_5 band or orbital of d_{yz} character.[42]

In even geometry there exist a number of Ag bands of Δ_1 symmetry, principally of s and $d_{3z^2-r^2}$ character in the vicinity of 6.9 eV binding energy.[43–45] Indeed we observe a strong band in even-geometry photoemission at this binding energy. This band can only exist in even geometry and can readily mix with a Hg band of similar binding energy and appropriate symmetry. The Hg band with 7.2 eV binding energy at $\bar{\Gamma}$ possesses Δ_5 symmetry at $\bar{\Gamma}$. Away from $\bar{\Gamma}$, these bands can mix, so the mixing of the Δ_5 Hg band and a Δ_1 Ag band along the $\bar{\Gamma}$-to-$\bar{X}$ direction is not only possible but favorable given the proximity of the binding energies of these two bands. For one monolayer of Hg, the 7.2-eV Δ_5 symmetry band (at $\bar{\Gamma}$) cannot be observed in even geometry away from $\bar{\Gamma}$. We conclude that the Ag bands of Δ_1 symmetry hybridize sufficiently with this Hg Δ_5 band to either broaden the band or reduce the oscillator strength of the band sufficiently to preclude observing it. For two monolayers of Hg on Ag(100), the lack of symmetry of the new 7.2-eV binding-energy band about $\bar{X}$ in even geometry and the dependence of this band upon $k_\perp$ (electron perpendicular momentum vector) can be accounted for in two ways. If the overlayer is thick enough to exhibit bulk bands, the spectral features would, in principal, depend upon both $k_\parallel$ and $k_\perp$. Typically, four or more monolayers are required to observe bulklike behavior. Thus, a more likely explanation for the $k_\parallel$ and k dependence of the dispersion of this Hg band is that this Δ_5 Hg band is still affected by the Δ_1 Ag band for the two monolayers of Hg on Ag(100). The effect upon the Hg Δ_5 band, adding what is effectively a $d_{3z^2-r^2}$ orbital, is to distort the Hg state wave function, introducing an effective $k_\perp$ dependence.

A picture thus emerges, one that accounts for the observed data in even symmetry from one and two monolayers of Hg deposited on Ag(100). The bulklike behavior of the Hg-induced bands reflects Hg-to-Ag hybridization. The bulklike band-structure behavior of the Hg bands reflects the bulk band structure of the relevant Ag(100) bands. Hence, the band observed only with two monolayers of Hg on Ag(100) in the vicinity of 3 eV binding energy to E_F near $\bar{X}$ in even geometry is the Δ_1 Ag(100) band (of principally 5s character) hybridizing with the Δ_1 symmetry orbitals of Hg (again of mostly 6s character). This band also exhibits a dependence upon both $k_\parallel$ and $k_\perp$, as would be expected from the pronounced hybridization of Hg and Ag that is responsible for its creation.

In odd geometry, there are no Δ_1 bands and no observed Ag bands below approximately 6.0 eV binding energy (Figs. 10 and 11). Thus, there is little for *odd*-symmetry 7.2-, 8.0-, and 9.8-eV binding-energy Hg bands to hybridize with. The pronounced dispersion for the band at approximately 7.2 eV is a result of considerable hybridization between adjacent Hg atomic orbitals as previously discussed.

Despite the very weak chemical interaction between the Hg overlayer and the Ag(100) surface, the overlayer and substrate do hybridize to form a distinct interfacial band structure away from $\bar{\Gamma}$ in even geometry. The observed features are thus accounted for by a predominant Hg-Hg interaction and a significant Hg-Ag interaction in even geometry.

D. Formation of a bulk Hg band structure

Following the adsorption of five monolayers of Hg on Ag(100) at 89 K, the $p(1\times4)$ overlayer structure is formed. We have no conclusive proof that the $p(1\times4)$ structure is accompanied by development of an Hg bulk band structure. Nonetheless the electronic properties of the overlayer are quite different from the overlayer band structure of one and two monolayers of Hg on Ag(100).

Following the adsorption of five monolayers of Hg on Ag(100) at 89 K, the band structure of the Hg-induced features in odd geometry exhibits some photon energy dependence. This is in marked contrast to one and two monolayers of Hg which exhibit no $k_\perp$ (photon energy) dependence.

The third Hg feature ($\sim$7.2 eV binding energy at $\bar{\Gamma}$) is not observed to disperse symmetrically about $\bar{X}$ in odd geometry. Due to the dispersion of the three Hg-induced photoemission features across the surface Brillouin zone has been plotted in Fig. 11. The band at approximately 7.2 eV binding energy at $\bar{\Gamma}$ disperses to greater binding with increasing momentum vector parallel with the surface $k_\parallel$. Due to the dispersion of this band to greater binding energies, together with the fading intensity away from $\bar{\Gamma}$, we found that the presence of the band is difficult

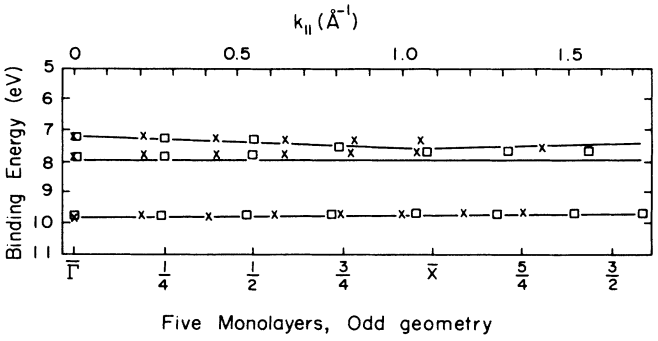

FIG. 11. The experimental band structure for five monolayers of Hg on Ag(100) at 89 K in odd geometry. The structure is the $p(1\times4)$ plus the $p(4\times1)$ (see text). Only the three Hg bands are shown for odd geometry from $\bar{\Gamma}$ to $\bar{X}$ of the surface Brillouin zone. The solid lines indicate the band structure for one and two monolayers of Hg, while x indicates the data taken for 36 eV photon energy and □ indicates the data taken for 50 eV photon energy.

to ascertain near $\bar{X}$. The dispersion back to lower binding energies and restoration of intensity of the band at ~ 7.2 eV does not occur in the next surface Brillouin zone.

Also, in contrast to one and two monolayers of Hg on Ag(100) where the band at approximately 7.2 eV binding energy increased in intensity from $\bar{\Gamma}$ to $\bar{X}$ (Fig. 8) for five monolayers of Hg on Ag(100) the intensity of this band was observed to decrease from $\bar{\Gamma}$ to $\bar{X}$.

There is little doubt that five monolayers of Hg do have a band structure. Despite the change of the overlayer crystal structure to the $p(1\times4)$, the close proximity of the Hg atoms in the overlayer net is maintained if either of the proposed overlayer structures for the $p(1\times4)$ is accepted. Further evidence of the Hg-atom hybridization is provided by the relative photoemission cross sections discussed in detail elsewhere.[12,46]

The change of the overlayer crystal structure from 1×1 for one and two monolayers of Hg to $p(1\times4)$ domains for five monolayers of Hg makes the band structures for thick and thin overlayers difficult to compare. Nonetheless, for some (50%) domains the 2.889 Å lattice spacing will be in the appropriate direction to provide a dispersion that, while perhaps not identical, is at least similar to the dispersion of the Hg bands observed with the $p(1\times4)$ in odd geometry. This, of course, assumes that one of the postulated solutions to the $p(1\times4)$ is correct and that the dispersion is a result, to a large extent, of the close Hg-Hg atom proximity. The domains which have the large lattice spacing in the appropriate direction will exhibit a band structure with little dispersion. This band structure will be superimposed upon a band structure with far greater dispersion from domains with a small lattice spacing in the same direction. Because of the significant interaction with the Ag(100) surface in even geometry, there is some difficulty in investigating the development of a bulk band structure for the Hg overlayer in increasing thickness. The Hg band at approximately 7.2 eV binding energy does not exhibit any hybridization with the Ag(100) surface in odd geometry for one and two monolayers of Hg. The development of bulklike band structure behavior in odd geometry for five monolayers of Hg is therefore unlikely to be a result of the influence of the Ag(100) substrate. Thus with five monolayers of Hg on Ag(100), we are beginning to see the development of a bulk Hg band structure. This result is by no means unequivocal. There is no dispersion within the accuracy of our measurements with changing photon energy at $\bar{\Gamma}$ (normal emission) for five monolayers of Hg on Ag(100). This implies that while a rudimentary bulk band structure may exist with five monolayers of Hg on Ag(100), this bulk band structure is far from fully developed. A similar development of bulk band structure has been observed for Ag deposited on Cu(100) for a five-monolayer overlayer.[47]

The photon energy dependence (dependence upon $k_\perp$) of the Hg bands and the lack of symmetric dispersion about $\bar{X}$ in odd geometry suggest that there is a rudimentary development of a bulk band structure for five monolayers of Hg on Ag(100). The changing photoemission intensity of the third Hg band (with 7.2 eV binding energy at $\bar{\Gamma}$) along $\bar{\Gamma}$ to $\bar{X}$ is consistent with a bulk band structure as well.

IV. CONCLUSION

The adsorption of one and two monolayers of Hg on Ag(100) at 89 K results in the formation of a new ordered face-centered-cubic crystal phase. This phase grows via a Frank–van der Merwe growth mode and is metastable as confirmed by our measurements and by calculations.[25–27,29]

This face-centered-cubic phase possesses an itinerant electronic band, arising predominantly from Hg-Hg interactions of $5d$ states. The Hg-Hg interactions may in part be attributable to the biaxial compression the Hg undergoes in forming this new phase on Ag(100).

The Ag(100), in addition to functioning as a structural template, hybridizes somewhat with the Hg overlayer but only in even geometry and away from $\bar{\Gamma}$ in the surface Brillioun zone. This occurs despite the small heat of adsorption of Hg on Ag(100). Interfacial states are observed with unusual properties that cannot be associated with conservation of two-dimensionality of state as would be expected.

As noted above, there exists evidence that the second phase of Hg on Ag(100) (five monolayers of Hg) exhibits some of the characteristics of a bulk band structure. These results are, however, inconclusive. As reported elsewhere, the second $[p(1\times4)]$ Hg overlayer phase also exhibits interesting and unexpected many-electron effects which appear to be the result of the itinerant band structure.[12]

ACKNOWLEDGMENTS

We would like to thank the staff of the Synchrotron Radiation Center of the University of Wisconsin, Madison. This facility is supported by Grant No. DMR-80-20164 from the National Science Foundation (NSF). The work has been aided by conversations with Dr. Leonard Kleinman and Dr. Art Williams. We would also like to thank Dr. Jack Gay for providing the details of his calculations for Ag(100). This work was supported by Syracuse University and the NSF through Grant No. DMR-83-04368.

*Present address: Department of Physics, University of Wisconsin, Madison, Wisconsin 53706

[1]E. Bauer, in *Interfacial Aspects of Phase Transformations,* edited by B. Mutafschiev (Riedel, Boston, 1982), p. 411.

[2]C. M. Falco and I. K. Schuller, in *Synthetic Modulated Structures,* edited by L. L. Change and B. C. Giessen (Academic, New York, 1985), p. 339.

[3]*Phase Transitions in Surface Films,* edited by J. G. Dash and J. Rubalds (Plenum, New York, 1979).

[4]S. T. Ruggiero and M. R. Beasly, in *Synthetic Modulated Struc-*

tures, edited by L. L. Change and B. C. Giessen (Academic, New York, 1985).
[5]B. D. Tonner, H. Li, M. J. Robrecht, Y. C. Chou, M. Onellion, and J. L. Erskine, Phys. Rev. B **34**, 4386 (1986).
[6]E. Bauer, Appl. Surf. Sci. **11/12**, 479 (1982).
[7]F. J. Himpsel, U. O. Karlsson, J. F. Morar, D. Rieger, and J. A. Yarmoff, Phys. Rev. Lett. **56**, 1497 (1986).
[8]C. R. Fuselier, J. C. Raich, and N. S. Gillis, Surf. Sci. **92**, 667 (1980).
[9]S. D. Kevan, N. G. Stoffel, and N. V. Smith, Phys. Rev. B **32**, 5038 (1985).
[10]R. Miranda, F. Yndurain, D. Chandesris, D. Lecante, and Y. Petroff, Phys. Rev. B **25**, 257 (1982).
[11]A. M. Donoho and J. L. Erskine, Phys. Rev. B **29**, 2986 (1984).
[12]Shika Varma, Y. J. Kime, P. A. Dowben, M. Onellion, and J. L. Erskine, Phys. Lett. **116A**, 66 (1986).
[13]G. K. Ovrebo and J. L. Erskine, J. Electron Spectrosc. Relat. Phenom. **24**, 189 (1981).
[14]M. Onellion, P. A. Dowben, and J. L. Erskine (unpublished).
[15]R. G. Jones and D. L. Perry, Surf. Sci. **71**, 59 (1978).
[16]R. G. Jones and D. L. Perry, Surf. Sci. **82**, 540 (1979).
[17]R. G. Jones and D. L. Perry, Vacuum **31**, 493 (1981).
[18]C. R. Brundle and M. W. Roberts, Proc. R. Soc. London, Ser. A **331**, 383 (1972).
[19]M. D. Seah and W. A. Dench, Surf. Int. Anal. **1**, 2 (1979).
[20]D. R. Penn, J. Electron Spectrosc. Relat. Phenom. **9**, 29 (1976).
[21]C. J. Powell, Surf. Sci. **44**, 29 (1974).
[22]J. H. van der Merwe, Thin Solid Films **74**, 129 (1980); F. C. Frank and J. van der Merwe, Proc. R. Soc. London, Ser. A **198**, 205 (1949); J. H. van der Merwe, Philos. Mag. A **45**, 127 (1982); **45**, 145 (1982); **45**, C59 (1982).
[23]I. Markov, and R. Kaishew, Krist. Tech. **11**, 685 (1976); Thin Solid Films **32**, 163 (1976).
[24]N. D. H. Ross and J. S. Abell, Phys. Status Solidi A **1**, K33 (1970); J. Donohue, *The Structure of the Elements* (Wiley, New York, 1974).
[25]D. Weaire, Philos. Mag. **18**, 213 (1968).
[26]V. Heine and D. Weaire, Phys. Rev. **152**, 603 (1966).
[27]D. Weaire, J. Phys. C **1**, 210 (1968).
[28]A. G. Crocker, F. Heckscher, M. Bevis, and D. M. M. Guyoncourt, Philos. Mag. **13**, 1191 (1966).
[29]J. Worster and N. H. March, Solid State Commun. **2**, 245 (1964).
[30]A. Sepulveda and G. E. Rhead, Surf. Sci. **66**, 436 (1977).
[31]R. E. Jones and A. W.-L. Tong, Surf. Sci. (to be published).
[32]S. Svensson, N. Mortensson, E. Basilier, P. A. Malmquist, U. Gelius, and K. Siegbahn, J. Electron Spectrosc. Relat. Phenom. **9**, 51 (1976).
[33]R. W. Joyner *et al.*, Surf. Sci. **87**, 507 (1979).
[34]G. E. Becker and H. G. Hagstrum, J. Vac. Sci. Technol. **10**, 31 (1973).
[35]W. F. Egelhoff, D. L. Perry, and J. W. Linnett, Surf. Sci. **54**, 670 (1976).
[36]J. L. Dehnmer and J. Berkowitz, Phys. Rev. A **10**, 484 (1974).
[37]Shin-ichi Ishi and Y. Ohno, Surf. Sci. **133**, L465 (1983).
[38]H. A. Bethe, Ann. Phys. (Leipzig) **5**, 133 (1929).
[39]J. F. Herbst, Phys. Rev. B **15**, 3720 (1977).
[40]M. Onellion, J. L. Erskine, Y. J. Kime, Shikha Varma, and P. A. Dowben, Phys. Rev. B **33**, 8833 (1986).
[41]F. J. Himpsel *et al.*, Phys. Rev. B **22**, 4604 (1980).
[42]N. V. Richardson and A. M. Bradshaw, in *Electron Spectroscopy—Theory, Techniques, and Application,* edited by C. R. Brundle and A. D. Baker (Academic, New York, 1981), Vol. 4; N. V. Richardson, Surf. Sci. **126**, 337 (1983); J. Hermanson, Solid State Commun. **22**, 9 (1977); M. Scheffler, K. Kambe, and F. Forstmann, *ibid.* **25**, 93 (1978).
[43]J. R. Smith, J. Gay, and F. J. Arlinghaus, Phys. Rev. B **21**, 2201 (1980).
[44]J. R. Smith, F. J. Arlinghaus, and J. G. Gay, Phys. Rev. B **22**, 4757 (1980).
[45]H. F. Roloff and Neddermeyer, Solid State Commun. **21**, 561 (1977).
[46]M. Onellion, P. A. Dowben, Y. J. Kime, and Shikha Varma (unpublished).
[47]J. G. Tobin, S. W. Robey, L. E. Klebanoff, and D. A. Shirley, Phys. Rev. B **28**, 6169 (1983).